

# Oxide Thin Film Transistor Circuits for Transparent RFID Applications

Seung Hyun CHO<sup>†</sup>, Sang Woo KIM<sup>†</sup>, Woo Seok CHEONG<sup>††</sup>, Chun Won BYUN<sup>††</sup>, Chi-Sun HWANG<sup>††</sup>,  
Kyoung Ik CHO<sup>††</sup>, and Byung Seong BAE<sup>†a)</sup>, Nonmembers

**SUMMARY** Oxide material can make transparent devices with transparent electrodes. We developed a transparent oscillator and rectifier circuits with oxide TFTs. The source/drain and gate electrodes were made by indium thin oxide (ITO), and active layer made by transparent material of IGZO (Indium Gallium Zinc Oxide) on a glass substrate. The RC oscillator was composed of bootstrapped inverters, and 813 kHz oscillation frequency was accomplished at  $V_{DD} = 15$  V. For DC voltage generation from RF, transparent rectifier was fabricated and evaluated. This DC voltage from rectifier powered to the oscillator which operated successfully to create RF. For data transmission, RF transmission was evaluated with RF from the transparent oscillator. An antenna was connected to the oscillator and RF transmission to a receiving antenna was verified. Through this transmission antenna, RF was transmitted to a receiving antenna successfully. For transparent system of RFID, transparent antenna was developed and verified sending and receiving of data.

**key words:** oxide TFT, oscillator, rectifier, transparent device, RF transfer

## 1. Introduction

Transparent electronics, an emerging technology, has attracted many interests, for it can open new applications for consumer electronics, transportation, business and military. The various applications can be suggested including display backplane, sensor, RF identification (RFID), smart card and etc. Among them, transparent display with communication function is a future display technology. RFID itself is also a very popular technology for an increasing number of applications.

Since amorphous silicon, organic thin-film transistor or oxide thin film transistor (TFT) can be manufactured using low-cost processes, they are adequate for low-cost circuits. For transparent system, oxide thin film transistor is preferable device due to its transparency and relatively large mobility compared to amorphous silicon and organic TFTs.

An oxide TFT has simple fabrication process and low leakage current like a-Si:H TFTs. Moreover, mobility is much larger than an a-Si:H TFT [1]–[3]. Therefore, transparent and low cost RFID is one of the applications of oxide TFT.

In RFID system, radio frequency is necessary for transmission of data. An oscillator, which is a basic unit for operations of most of electronic systems, is used for gen-

eration of RF and there is an increasing technological interest in radio frequency application. Circuits with TFTs have been developed because of the demand for a low-cost RFID [4], [5]. RFID devices are generally being deployed in four main communication bands: the low-frequency range up to 135 kHz, a band at 13.56 MHz, a band at 900 MHz, and a band at 2.4 GHz [6], [7]. Among them, the low and the band at 13.56 MHz are adequate ranges of RFID with oxide TFTs. For low frequency range up to 135 kHz, amorphous silicon TFT oscillator achieved oscillation frequency of this low range [8]. With oxide TFTs, much higher frequencies were achieved [9].

For RFID applications, rectifier as well as oscillator is necessary to generate DC voltage for the operation of the circuit. We evaluated transparent rectifier which generate DC power from input RF.

For RF transmission, antenna is essential and should be transparent for transparent data transmission system. We evaluated transparent antenna with indium tin oxide (ITO) for data transmission with carrier RF. It was successful to transmit data with transparent antenna.

In this paper, we verified RC oscillator and rectifier using oxide TFTs. It was successful to transmit RF from the oscillator to a receiving antenna through a transmission antenna connected to the oscillator.

## 2. Experimental Details

Transparent oscillator and rectifier circuits were developed with oxide TFTs [10]. Figure 1 shows the cross-sectional structure of the fabricated oxide TFT with top gate structure. After deposition of a 150 Å  $\text{SiO}_2$  buffer layer on a glass substrate, ITO was deposited and patterned as source/drain (S/D) electrodes.

Active layer was a 200 Å indium-gallium-zinc-oxide (IGZO) by sputtering. After pattern of active layer, gate insulator was formed. We deposited an 90 Å Aluminum

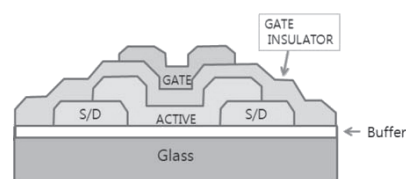


Fig. 1 Cross sectional structure of the fabricated oxide TFT.

Manuscript received April 19, 2010.

Manuscript revised June 2, 2010.

<sup>†</sup>The authors are with Hoseo University, Asan, 336-795, Korea.

<sup>††</sup>The authors are with ETRI, Daejeon, 305-350, Korea.

a) E-mail: bsbae3@hanmail.net

DOI: 10.1587/transele.E93.C.1504

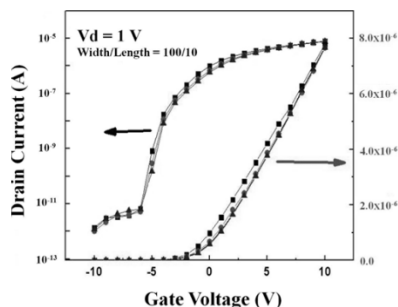


Fig. 2 Transfer curves of the fabricated oxide TFTs.

oxide layer as a protective layer before 1700 Å Aluminum oxide for 2nd gate insulator. On the gate insulator, 1500 Å gate electrode was formed with ITO. Figure 2 shows transfer characteristics of IGZO TFTs used for this study. The off current was  $10^{-12}$  A. An on/off current ratio was about  $10^7$  at  $V_D = 1$  V. Field effect mobility was  $6.7 \text{ cm}^2/\text{Vs}$ .

Since all the materials for the TFT and electrodes were transparent, fabricated oxide TFTs and circuits were transparent.

### 3. Oscillator and Rectifier

The schematic of the RC oscillator is shown in Fig. 3. The oscillator circuit is transparent and Fig. 4 shows microscope image of the circuit. The RC oscillator is composed of 3 stage inverters, a feed-back resistor and a capacitor. The inverter is bootstrap inverter as shown inside circle in Fig. 3. The frequency of an RC oscillator is decided by R, C and supply voltage as well as inverter characteristics. We measured the oscillation voltage without output buffer because inverter was designed to have enough high current for 10 pF input capacitance of an oscilloscope.

In a bootstrap inverter, the gate voltages of load transistor (TR) increase over  $V_{DD}$  due to bootstrapping though the bootstrap capacitor C and the parasitic capacitance of the load TR when the voltage of the output node becomes high. Due to overdrive of the load TFT, high voltage output at the output node can be as high as  $V_{DD}$ . Therefore, we can get improved inverter characteristics even with N-channel only TFTs.

A load transistor with length =  $10 \mu\text{m}$  and width =  $200 \mu\text{m}$ , drive transistor with length =  $10 \mu\text{m}$  and width =  $1600 \mu\text{m}$ , and capacitor =  $0.5 \text{ pF}$  were used for the bootstrapped inverter.

Figure 5 (a) shows output waveform of the RC oscillator when  $R = 1 \text{ k}\Omega$  and  $C = 1 \text{ pF}$  with supply bias ( $V_{DD}$ ) of 15 V. An oscillation frequency of 813 kHz was obtained with voltage swing from 1.5 V to 8 V. Figure 5(b) shows the RC oscillator output when  $R = 10 \text{ k}\Omega$  and  $C = 10 \text{ pF}$  with  $V_{DD} = 15$  V. An oscillation frequency of 164 kHz was obtained with voltage swing from 2 V to 7.5 V. Higher RC results in lower oscillation frequency. As measured above, oscillation frequencies can be adjusted by changing resistance and capacitance. And also, the oscillators were verified by observ-

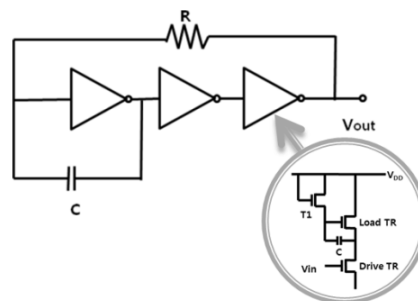


Fig. 3 Schematic of the RC oscillator with bootstrapped inverters.

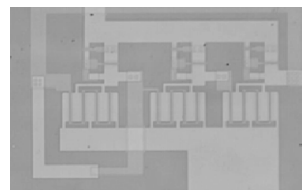
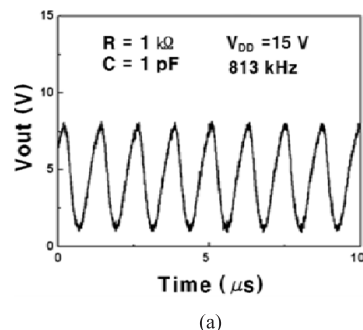
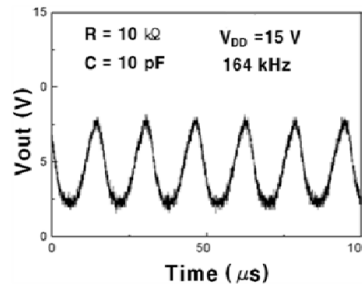


Fig. 4 Microphotograph of the fabricated RC oscillator.



(a)



(b)

Fig. 5 Oscillation output of the RC oscillator with  $R = 1 \text{ k}\Omega$  and  $C = 1 \text{ pF}$  (a), and with  $R = 10 \text{ k}\Omega$  and  $C = 10 \text{ pF}$  (b).

ing the increase of oscillation frequency with increasing of  $V_{DD}$ .

In the case of passive type tag in RFID, the DC voltage is generated from received RF for the operation of the circuits inside tag [5]. Therefore, rectifier is necessary to supply DC power to circuits. We fabricated two types of transparent rectifiers with IGZO oxide TFTs as shown in Fig. 6. One is half-wave rectifier and the other is voltage doubling rectifier.

Transistor with length =  $10 \mu\text{m}$ , width =  $2000 \mu\text{m}$ , and

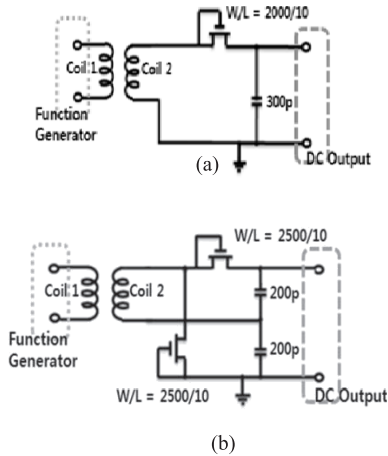


Fig. 6 Schematic of the half-wave rectifier (a), and voltage doubling rectifier (b).

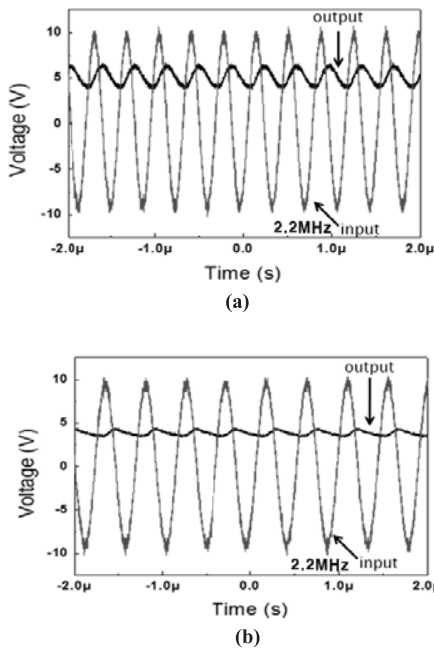


Fig. 7 AC input and DC output of the half-wave rectifier (a), and of the voltage doubling rectifier (b).

capacitor of  $300\text{pF}$  were used for the half-wave rectifier. Transistors with length =  $10\text{ }\mu\text{m}$ , width =  $2500\text{ }\mu\text{m}$  and capacitor of  $200\text{pF}$  were used for the voltage doubling rectifier. Function generator was used for supplying AC sine wave to the antenna coil 1. The voltage induced at the antenna coil 2 was rectified by transparent rectifier.

AC input to the coil 2 and DC output of the rectifier are shown in Fig. 7. Figure 7(a) is for half wave rectifier and Fig. 7(b) is for voltage doubling rectifier. The amplitude of AC input to the coil 1 was 10 V. Figure 7(a) shows about 5 V DC output and some ripple which means higher capacitance is necessary. Figure 7(b) shows about 4.8 V DC output and less ripple compared to the half wave rectifier. However, the voltage is not improved as we expected for voltage dou-

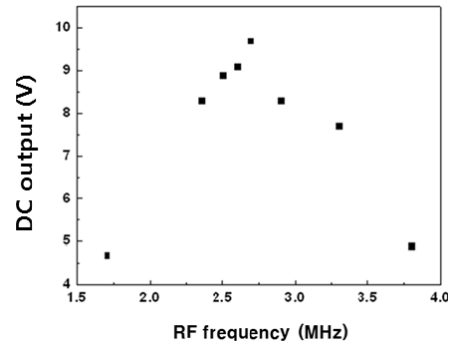


Fig. 8 We could get optimum input RF frequency which gave the highest DC output voltage.

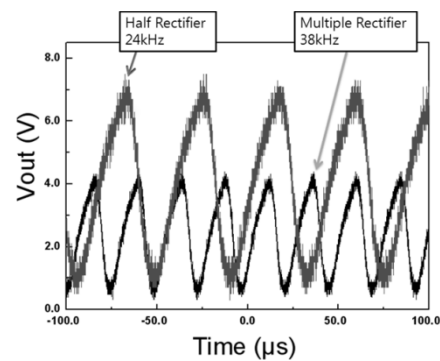


Fig. 9 Oscillation outputs with DC voltages from the rectifiers.

bling rectifier. It needs more investigation and one way to investigate of it would be to compare the resonance condition of combined circuits with antenna and rectifier circuits between half wave and voltage doubling rectifiers.

The coupling efficiency between the antenna coils and rectifying efficiency depend on input AC frequency. Figure 8 shows RF frequency dependence of the DC output of the half-wave rectifier. For high efficiency of power transmission, it is important to find out tuned condition. By tuning frequencies, we could get optimum RF frequency which gave the highest DC output voltage. At the frequencies of around 2.7 MHz, we could get about 9.5 V DC voltages.

We supplied DC voltage from the rectifier to the RC oscillator to check the operation of the oscillator with DC voltage form the rectifier. Figure 9 shows the operation of the oscillator with DC voltage from the rectifier.

Oscillator operates well with DC voltage from the half-wave rectifier. The oscillation voltage swing from 0.3 V to 7.0 V and the oscillation frequency was about 24 kHz. The low operation frequency is attributed to low DC voltage and not tuned condition in terms of frequency. To establish higher oscillation frequencies, it is necessary to improve rectifier efficiency by optimizing the circuit and tuning resonance condition. The swing of low frequency is larger than that of high frequency oscillation as shown in Fig. 9. The swing of the oscillation becomes smaller as increasing the oscillation frequencies because the feedback voltage arrives before the voltage changes completely due to long rise or

fall time compared to feedback time.

### 4. Transmission of Radio Frequency

We have developed the transparent RC oscillator and next task was to transmit the RF of the oscillator to a receiving antenna. We connected a transmission antenna to the oscillator and measured the received RF at a receiving antenna. The antennas were hand-wound copper coils.

The transmission antenna  $L_1$  was a part of LC oscillator with inverters as shown in Fig. 10(a). By the oscillation currents through the transmission antenna coil  $L_1$ , RF was transmitted to the receiving antenna  $L_2$ . The oscillation frequency of the RC oscillator is decided by the inverter characteristics, capacitances of each part and the inductances of coils. Oscillation waveform without the receiving antenna  $L_2$  is shown in Fig. 10(b). The oscillation frequency was 58 kHz at  $V_{DD} = 12$  V.

Since the transmission antenna coil  $L_1$  is in the feedback loop from output to the input of the first stage inverter, one of the factors that affect the frequency is the impedance of the inductance  $L_1$  and capacitance of  $C_1$ . Since these impedances depends on the frequency, to find out optimum value for the resonance is important to get high oscillation frequency. Moreover, at the resonance condition we can get highest current through the transmission antenna coil  $L_1$  which means highest RF power because the intensity of the induced magnetic field proportional to the current of coil. After put the receiving antenna coil  $L_2$  stacked to the transmission antenna coil  $L_1$ , we measured the output signal of the receiving antenna coil  $L_2$ .

Figure 11 shows signal when the receiving antenna coil  $L_2$  was put 1 cm apart from the transmission antenna coil  $L_1$ . The signal shows around 0.22 peak-to-peak volts. After 5 cm apart, signal shows about 0.10 peak to peak volts. The amplitude shows enough voltages to communicate each other even with 5 cm distance between two antennas.

### 5. Data Transmission with Transparent Antenna

We have established transparent circuits such as rectifier and oscillator. For data transmission, we accomplished the RF transmission with RF from transparent oscillator. However, the antennas used for transmission and receiving RF were copper coils which were not transparent. In terms of transparent antenna, there were reports on the antennas with conductive polymers [11], [12]. In this paper, we present an optically transparent antenna with ITO.

The antenna was one turn ITO square spiral pattern on a glass as shown in Fig. 12. The outer dimension of the antenna was  $5\text{ cm} \times 5\text{ cm}$ . We prepared two transparent antennas. One was for transmission and the other was for receiving. Since the ITO resistivity is larger compared to metals such as copper and aluminum, it is important to achieve enough low resistance of antenna. We minimized the resistance of the antenna by widening the width of the one turn square spiral pattern.

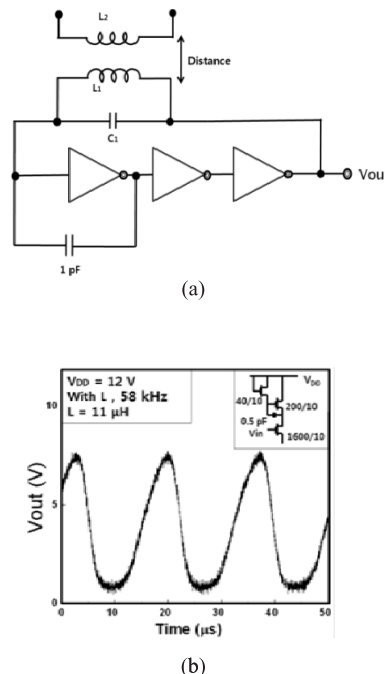


Fig. 10 The schematic of RF transmission experiment (a), and output wave form of the RC oscillator without  $L_2$  (b).

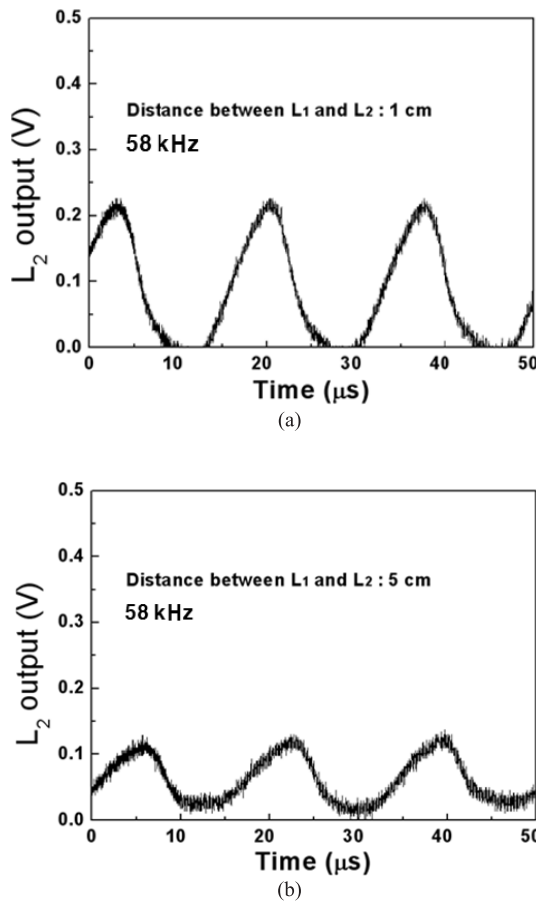
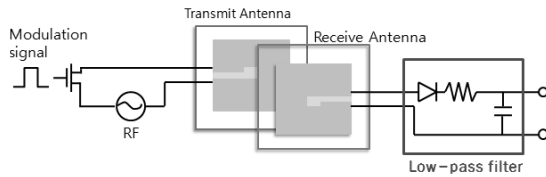
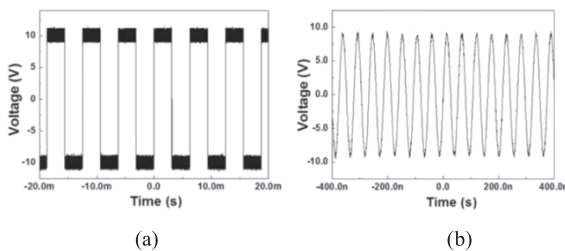


Fig. 11 The output signal at the receiving antenna coil  $L_2$  when the distance between  $L_1$  and  $L_2$  was 1 cm (a), and (b) shows the output signal at the receiving antenna coil  $L_2$  when the distance between  $L_1$  and  $L_2$  was 5 cm.



**Fig. 12** The verification of data transmission through the transparent antennas.



**Fig. 13** The left is the modulation signal of 160 Hz (a), and the right is the 18.7 MHz RF for transmission (b).

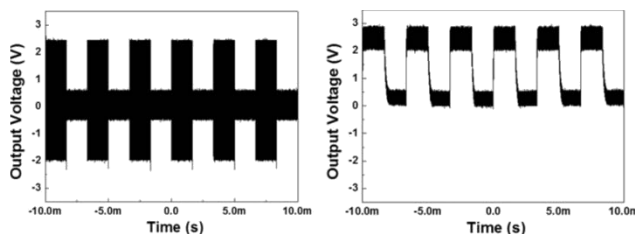


**Fig. 14** The left is the received modulated RF (a), and the right is after rectifying and passing the low pass filter (b).

To verify the transmission of data, we modulated the transmitting RF with modulation signal which is equivalent to data. Modulation signal was square wave, and input to the gate electrode of MOS FET to switch the connection of RF to the transmission antenna as shown in Fig. 12. The data to transmit to a receiver was this square wave and its frequency was 160 Hz. In practice, this square wave can be replaced by real data.

Figure 12 shows the verification of data transmission through the transparent antennas. The modulated RF was transmitted to the receiving antenna 1 mm apart from the transmission antenna. The received RF was rectified and passed the low pass filter to remove RF. After removing RF by low pass filter we could extract the original data transmitted. The data is square wave in this case.

Figure 13 shows the RF for transmission and square wave for modulation. The left is the modulation signal and the noise of the square wave was due to the interference by the RF. RF is shown at the right and its frequency was 18.7 MHz.

The transmission efficiency is much sensitive to RF frequencies due to resonance condition. We tuned the frequencies and obtained highest efficiency at the 18.7 MHz in the system shown in Fig. 12. With this frequency we could maximize the received signal at the receiving antenna.



**Fig. 15** The picture of the transparent ITO antenna. The outer dimension of the ITO antenna was 5 cm  $\times$  5 cm.

The received RF at the receiving antenna is shown in Fig. 14. The antenna used for this experiment is shown in Fig. 15. Since the RF was modulated by the modulation signal, received RF shows modulated form. To recover data transmitted we rectified the received RF at first. And then, the rectified signal was passed low pass filter to remove RF. The signal after low pass filter is shown at the right in Fig. 14. The original data of the square wave was successfully recovered.

## 6. Conclusions

We developed transparent rectifiers and oscillators with oxide TFTs and transparent electrodes. Input RF was rectified with developed transparent rectifier to DC voltage. The efficiency of the rectifier depends strongly on input RF frequency, for the developed rectifier tuned frequency was about 2.7 MHz with which the rectifier gave maximum DC voltage.

The transparent RC oscillator was developed and operated at oscillation frequency of 813 kHz with  $V_{DD} = 15$  V. With the DC voltage from the rectifier, we operated transparent RC oscillator. The measured oscillation frequency was 24 kHz.

The RF generated by transparent RC oscillator was transmitted to a receiving antenna through a transmission antenna which was connected to the feed-back loop of the RC oscillator. The RF signal was detectable at the receiving antenna. It was observed 0.1 V peak-to-peak signal even 5 cm distance between the receiving antenna and transmission antenna.

We developed transparent antenna for data transmission by minimizing the resistance of the square spiral ITO pattern. With developed transparent square spiral antenna, data transmission was successfully verified. With optimum integration of circuits, complete transparent RFID system can be achieved.

## Acknowledgments

This work was supported by IT R&D program of Ministry of Knowledge Economy. [2006-S079-02, Smart window with transparent electronic devices.]

## References

- [1] R.L. Hoffman, "ZnO-channel thin-film transistors: Channel mobility," *J. Appl. Phys.*, vol.95, no.10, pp.5813–5819, May 2004.

- [2] B. Yaglioglu, H.Y. Yeom, R. Beresford, and D.C. Painea, "High-mobility amorphous  $\text{In}_2\text{O}_3$ -10 wt%ZnO thin film transistors," *J. Appl. Phys. Lett.*, vol.89, pp.62103-1-62103-3, 2006.
- [3] R.B. M. Cross, M. Merlyne De Souza, S.C. Deane, and N.D. Young, "A comparison of the performance and stability of ZnO-TFTs with silicon dioxide and nitride as gate insulators," *IEEE Trans. Electron Devices*, vol.55, no.5, pp.1109-1115, May 2008.
- [4] P.F. Baude, D.A. Ender, M.A. Haase, T.W. Kelley, D.V. Muyres, and S.D. Theiss, "Pentacene-based radio-frequency identification circuitry," *Appl. Phys. Lett.*, vol.82, no.22, pp.3964-3966, June 2003.
- [5] E. Cantatore, T.C.T. Geuns, G.H. Gelinck, Erik van Veenendaal, A.F.A. Gruijthuisen, L. Schrijnemakers, S. Drews, and D.M. de Leeuw, "A 13.56-MHz RFID system based on organic transponders," *IEEE J. Solid-State Circuits*, vol.42, no.1, pp.84-92, Jan. 2007.
- [6] T. Scharfeld, An analysis of the fundamental constraints on low-cost passive radio-frequency identification system design, M.S. Thesis, Mass. Inst. of Technol., Cambridge, MA, 2001.
- [7] V. Subramanian, P.C. Chang, J.B. Lee, S.E. Molesa, and S.K. Volkman, "Printed organic transistors for ultra-low-cost RFID applications," *IEEE Trans. Compon. Packag. Manuf. Technol.*, vol.28, no.4, pp.742-747, Dec. 2005.
- [8] B.S. Bae, J.W. Choi, S.H. Kim, J.H. Oh, and J. Jang, "Stability of an amorphous silicon oscillator," *ETRI Journal*, vol.28, no.1, pp.46-50, Feb. 2006.
- [9] J. Sun, D.A. Mourey, D. Zhao, S.K. Park, S.F. Nelson, D.H. Levy, D. Freeman, P. Cowdery-Corvan, L. Tutt, and T.N. Jackson, "ZnO thin-film transistor ring oscillators with 31-ns propagation delay," *IEEE Electron Device Lett.*, vol.29, no.7, pp.721-723, July 2008.
- [10] S.H. Ko Park, D.H. Cho, C.S. Hwang, S. Yang, M.K. Ryu, C.W. Byun, S.M. Yoon, W.S. Cheong, K.I. Cho, and J.H. Jeon, "Channel protection layer effect on the performance of oxide TFTs," *ETRI Journal*, vol.31, no.6, pp.653-659, Dec. 2009.
- [11] S. Cichos, J. Haberland, and H. Reichl, "Performance analysis of polymer based antenna-coils for RFID," 2002 IEEE Conference on Polymers and Adhesives in Microelectronics and Photonics, pp.120-124, 2002.
- [12] N.J. Kirsch, N.A. Vacirca, E.E. Plowman, T.P. Kurzweg, A.K. Fontecchio, and K.R. Dandekar, "Optically transparent conductive polymer RFID meandering dipole antenna," 2009 IEEE International Conference on RFID, pp.278-282, 2009.



**Seung Hyun Cho** was born in Asan, Korea, in 1982. He received the B.S. degree from display engineering of the Hoseo University, Asan, Korea, in 2009. He is pursuing the M.S. degree in display engineering at the Hoseo university. His current research interest is oxide device and transparent RFID.



**Sang Woo Kim** was born in Seoul, Korea, in 1981. He received the B.S. and M.S. degree in display engineering from the Hoseo University, Asan, Korea, in 2007, and 2010, respectively.



**Woo Seok Cheong** received the B.S. degree from Yonsei University, Seoul, Korea, in 1992, and the M.S. and Ph.D. degrees from Korea Advanced Institute of Science and Technology (KAIST), Daejeon, Korea, in 1994 and 1998. During his doctoral course, his research focused on charge-related deposition phenomenon in chemical vapor deposition (CVD) and selective epitaxial growth (SEG). From 1998 to 2001, he was with Hyundai Electronics Inc. In 2002, he joined ETRI. His major interests are fabrication of nano-size electronic devices, tunneling magneto-resistance (TMR) sensors in hybrid magnetic recording system, carbon nanotubes, transparent conductive oxides, ionized physical vapor deposition equipment, new oxides semiconductors, flexible transistors, and highly stable oxide thin-film transistors. Currently, he is preparing the realization of transparent displays for car-navigation.



**Chun Won Byun** received the B.S. and the M.S. degrees in electrical and computer engineering from Hanyang University, Seoul, Korea, in 2002 and 2007, respectively. In 2007, he joined Transparent Display Team, ETRI (Electronics and Telecommunications Research Institute), Daejeon, Korea. His research interests include the transparent electronics and driving methods, circuits for flat panel displays.



**Chi-Sun Hwang** received the B.S. degree from Seoul National University in 1991 and the Ph.D. degrees from Korea Advanced Institute of Science and Technology in 1996, both in physics. From 1996 to 2000, he worked to make DRAM device with  $0.18\ \mu\text{m}$  technology at Hyundai Semiconductor Inc. Since he joined ETRI in 2000, he has been involved in flat panel display research, such as active-controlled field emission display, OLED and transparent display with oxide thin-film transistors.



**Kyoung Ik Cho** received the B.S. degree in Materials Science from Ulsan Institute of Technology in 1979, and the M.S. and Ph.D. degrees in Material Science and Engineering from Korea Advanced Institute of Science and Technology, in 1981 and 1991, respectively. He joined the Electronics and Telecommunications Research Institute (ETRI) in 1981. He has been working on the development of advanced display devices, and new electronic devices and materials. His current research interests include oxide TFT

and transparent display, and flexible electronic devices.



**Byung Seong Bae** received the B.S. degree in atomic nuclear engineering from the Seoul National University, Seoul, Korea, in 1984 and the M.S. and Ph.D. degrees in applied physics from the Korea Advanced Institute of Science and Technology, Seoul, in 1986, and 1991, respectively. Between 1991 and 1998, he worked at the Samsung Electronics on the development of amorphous and poly-silicon TFT LCD with integrated driver. From 1999 to 2003, he set up the high-temperature poly-silicon TFT LCD

factory and developed micro-display for projection display at ILJIN Display. Since 2006, he is a professor, School of Display Engineering of the Hoseo University, Asan, Korea.